Pharmacophore Modeling and *in Silico* Toxicity Assessment of Potential Anticancer Agents from African Medicinal Plants

Fidele Ntie-Kang [1,2,*¶], Conrad Veranso Simoben [2¶], Berin Karaman [1], Valery Fuh Ngwa [3], Philip Neville Judson [4], Wolfgang Sippl [1], Luc Meva'a Mbaze [5,*]

[1] Department of Pharmaceutical Chemistry, Martin-Luther University of Halle-Wittenberg, Wolfgang-Langenbeck Str. 4, 06120, Halle Saale, Germany

[2] Department of Chemistry, University of Buea, P. O. Box 63, Buea, Cameroon

[3] Leuven Biostatistics and Statistical Bioinformatics Centre, Universiteit Hasselt, Russelbeekstraat 27, 3590-Diepenbeek, Hasselt, Belgium

[4] Chemical Bioactivity Information Centre, Heather Lea, Bland Hill, Norwood, Harrogate HG3 1TE, UK.

[5] Department of Chemistry, Faculty of Science, University of Douala, P. O. Box 24157, Douala, Cameroon

* Corresponding authors

E-mail: ntiekfidele@gmail.com or fidele.ntie-kang@ubuea.cm (FNK); E-mail: lmbazze@yahoo.fr (LMM);

SUPPORTING INFORMATION

List S1: List of Toxicity Endpoint Considered by Lhasa's Derek Nexus in this Study:

alpha-2-mu-Globulin nephropathy, Anaphylaxis, Bladder urothelial hyperplasia, Carcinogenicity, Cardiotoxicity, Cerebral oedema, Chloracne, Cholinesterase inhibition, Chromosome damage in vitro, Chromosome damage in vivo, Cumulative effect on white cell count and immunology, Cyanide-type effects, Developmental toxicity, Genotoxicity in vitro, Genotoxicity in vivo, Hepatotoxicity, HERG channel inhibition in vitro, High acute toxicity, Irritation (of the eye), Irritation (of the gastrointestinal tract), Irritation (of the respiratory tract), Irritation (of the skin), Lachrymation, Methaemoglobinaemia, Mutagenicity in vitro, Mutagenicity in vivo, Nephrotoxicity, Neurotoxicity, Occupational asthma, Ocular toxicity, Oestrogenicity, Peroxisome proliferation, Phospholipidosis, Photo-induced chromosome damage in vitro, Photoallergenicity, Photocarcinogenicity, Photogenotoxicity in vitro, Photogenotoxicity in vivo, Photomutagenicity in vitro, Phototoxicity, Pulmonary toxicity, Rapid prototypes: adrenal gland toxicity, Rapid prototypes: bladder disorders, Rapid prototypes: blood in urine, Rapid prototypes: bone marrow toxicity, Rapid prototypes: bradycardia, Rapid prototypes: cardiotoxicity, Rapid prototypes: chromosome damage in vitro, Rapid prototypes: hepatotoxicity, Rapid prototypes: kidney disorders, Rapid prototypes: mitochondrial dysfunction, Rapid prototypes: nephrotoxicity, Rapid prototypes: splenotoxicity, Rapid prototypes: testicular toxicity, Rapid prototypes: thyroid toxicity,

Respiratory sensitisation, Skin sensitisation, Teratogenicity, Testicular toxicity, Thyroid toxicity, Uncoupler of oxidative phosphorylation.

Table S1: Definitions of likelihoods of Derek predictions

CERTAIN	There is proof that the proposition is true
PROBABLE	There is at least one strong argument that the proposition is true and there are no arguments against it
PLAUSIBLE	The weight of evidence supports the proposition
EQUIVOCAL	There is an equal weight of evidence for and against the proposition
DOUBTED	The weight of evidence opposes the proposition
IMPROBABLE	There is at least one strong argument that the proposition is false and there are no arguments for it
IMPOSSIBLE	There is proof that the proposition is false

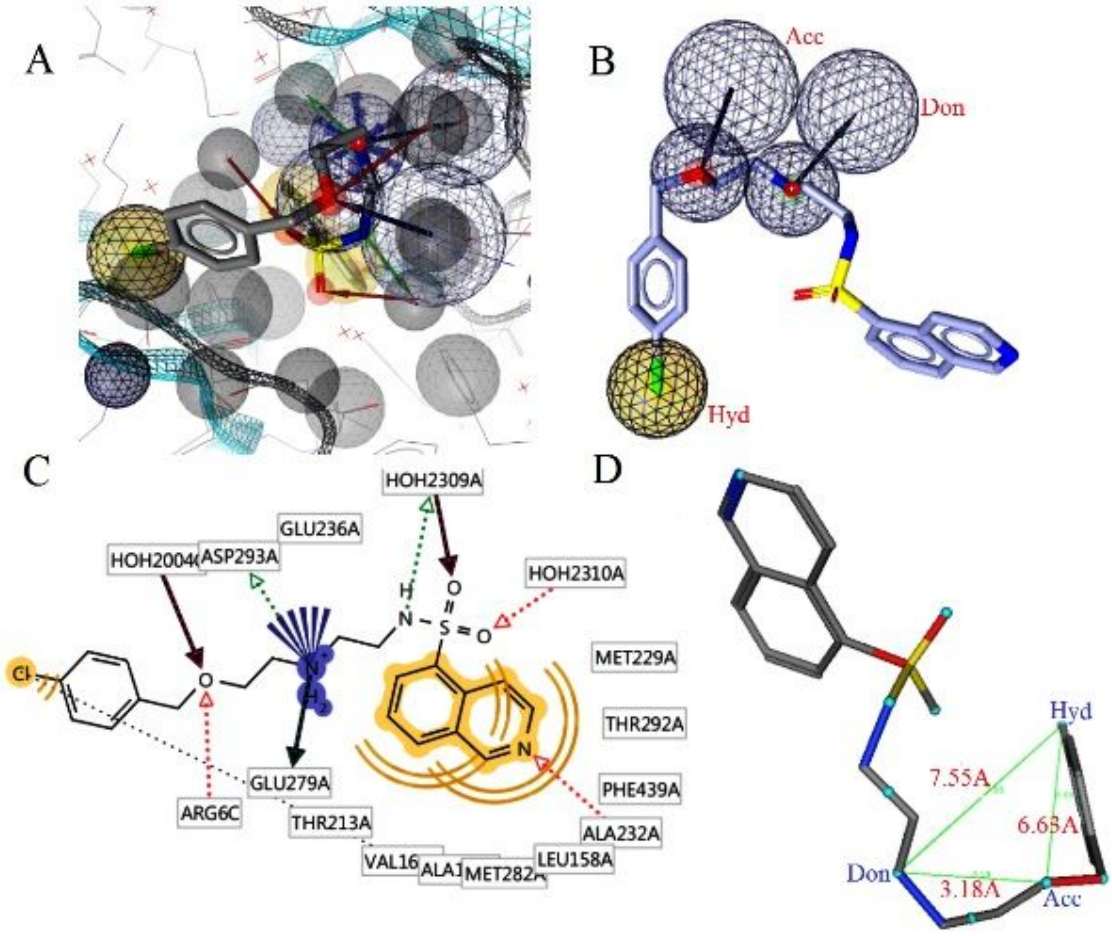

Figure S1. Pharmacophore model used to screen for potential active compounds against the 2JDO target; (A) projected within the target site, (B) with highlighted pharmacophore features located on atomic centers of the native ligand, H-bond donors and acceptors in blue and hydrophobic centers in yellow, (C) interactions between native ligand and target site amino acid residues, with hydrophobic interactions shown in light brown, H-bond donor interactions with the native ligand in green and acceptor interactions in red, (D) locations of centers of pharmacophore features on the native ligand showing distances between the centers, with distance measurements shown in red.

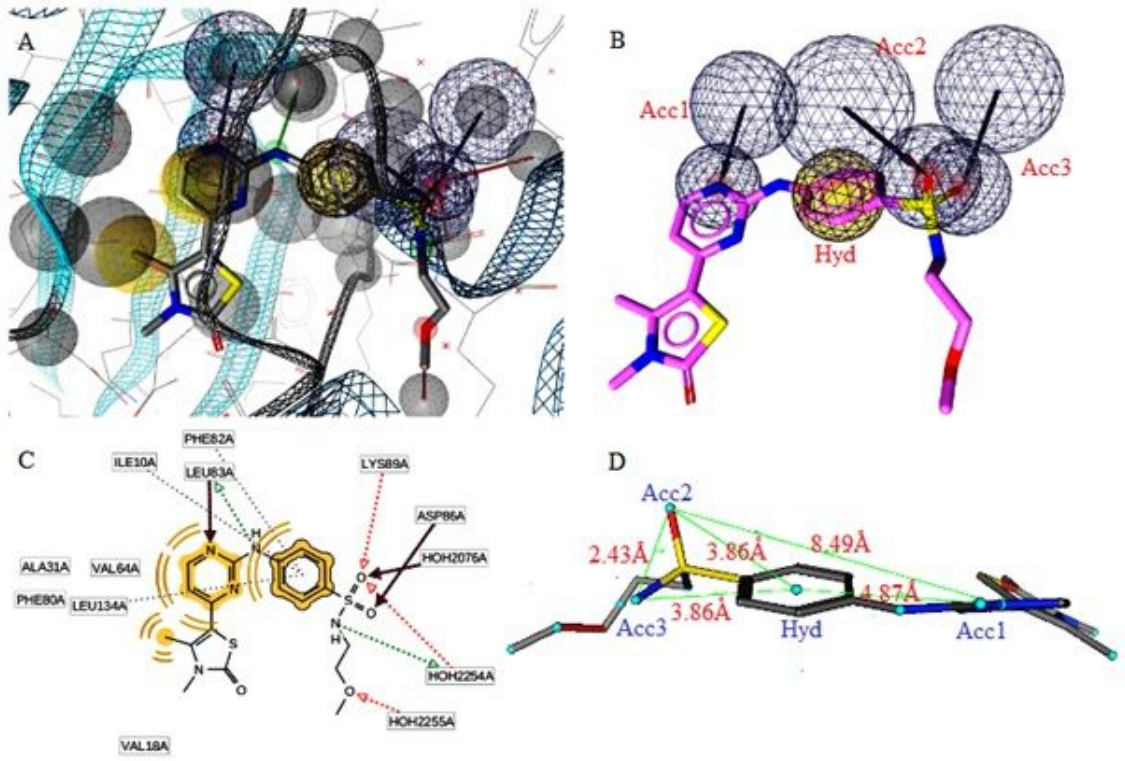

Figure S2. Pharmacophore model used to screen for potential active compounds against the 2XMY target; (A) projected within the target site, (B) with highlighted pharmacophore features located on atomic centers of the native ligand, H-bond donors and acceptors in blue and hydrophobic centers in yellow, (C) interactions between native ligand and target site amino acid residues, with hydrophobic interactions shown in light brown, H-bond donor interactions with the native ligand in green and acceptor interactions in red, (D) locations of centres of pharmacophore features on the native ligand showing distances between the centers, with distance measurements shown in red.

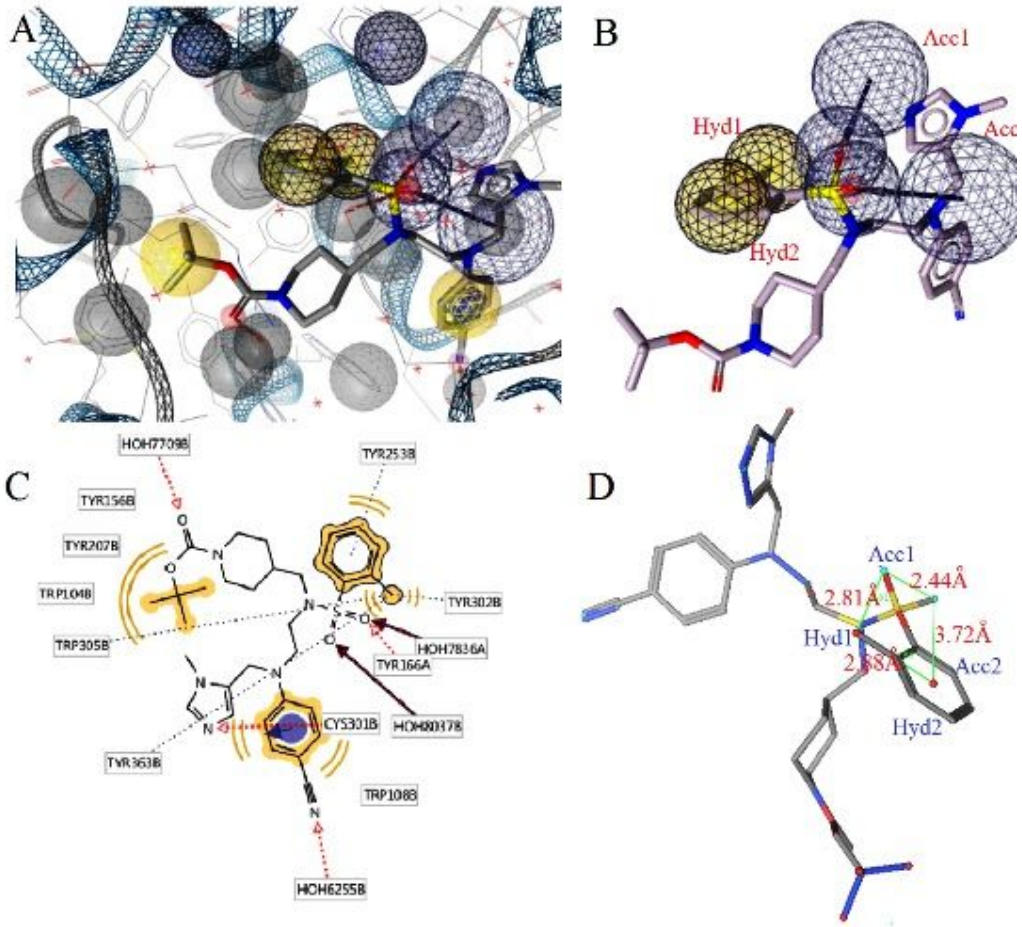
A
B
Acc1
Hyd1
Hyd2
C
HOH7709B
TYR253B
TYR156B
TYR207B
TRP104B
TYR302B
TRP305B
HOH7836A
TYR166A
CYS301B
HOH8078
TYR363B
TRP108B
HOH6255B
D
Acc1
2.44Å
2.81Å
Hyd1
3.72Å
Acc2
Hyd2

(I)

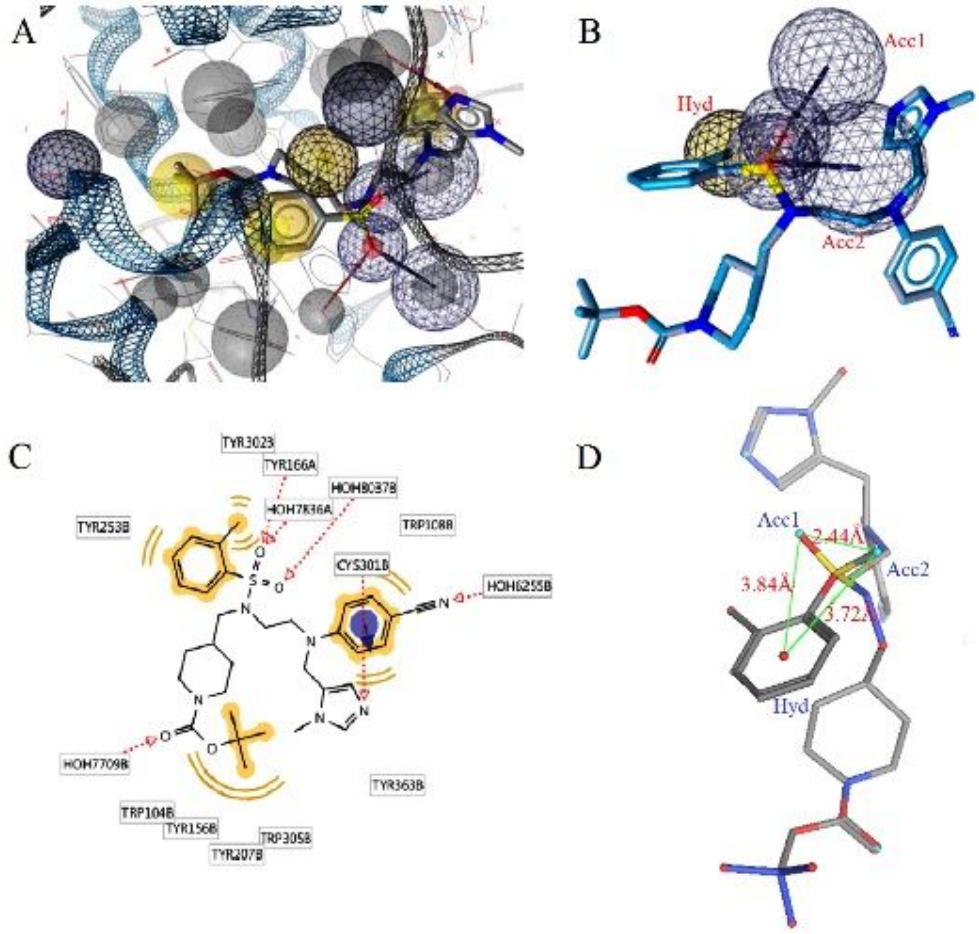
A
B
Acc1
Hyd
Acc2
C
TYR302B
TYR166A
HOH8037B
HOH7836A
TYR253B
TRP108B
CYS301B
HOH6255B
HOH7709B
TYR363B
TRP104B
TYR156B
TRP305B
TYR207B
D
Acc1
2.44Å
Acc2
3.84Å
3.72Å
Hyd

(II)

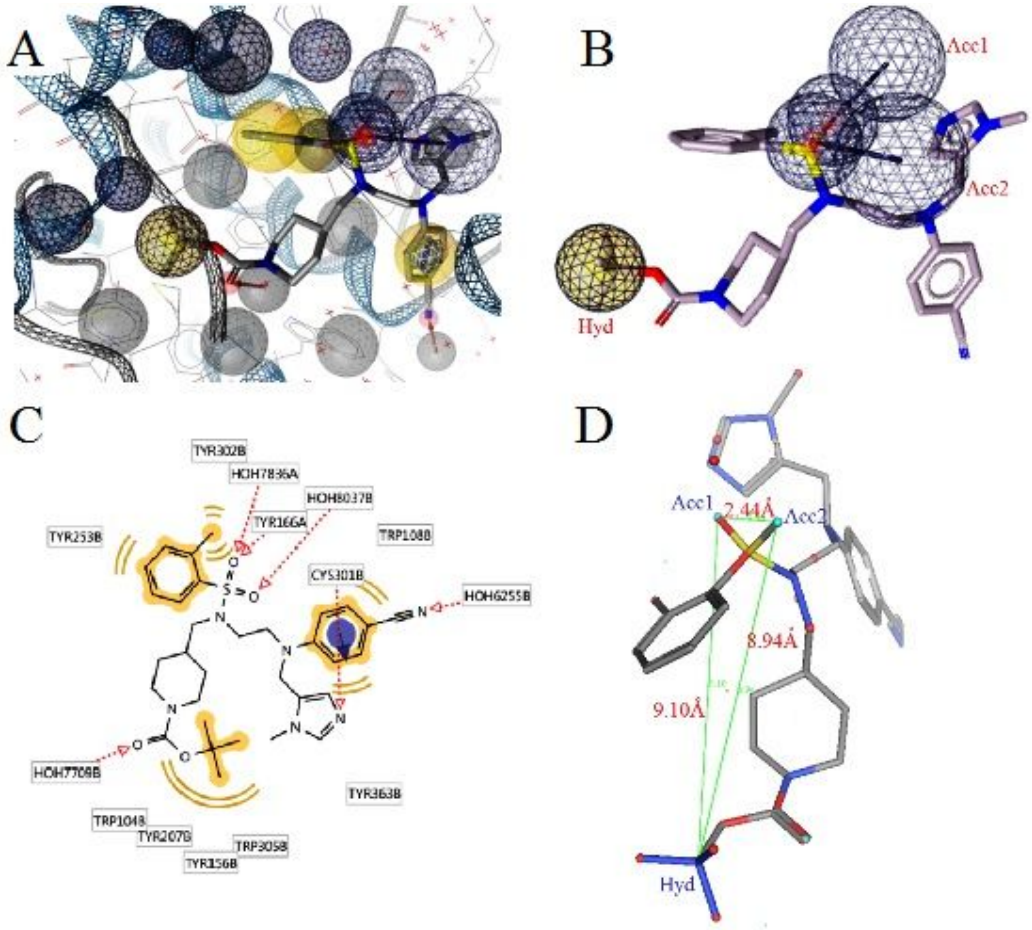

(III)

Figure S3. (I) 3E37 Model I, (II) 3E37 Model II, (III) 3E37 Model III

Pharmacophore models used to screen for potential active compounds against the 3E37 target; (A) projected within the target site, (B) with highlighted pharmacophore features located on atomic centres of the native ligand, H-bond donors and acceptors in blue and hydrophobic centers in yellow, (C) interactions between native ligand and target site amino acid residues, with hydrophobic interactions shown in light brown, H-bond donor interactions with the native ligand in green and acceptor interactions in red, (D) locations of centers of pharmacophore features on the native ligand showing distances between the centers, with distance measurements shown in red.

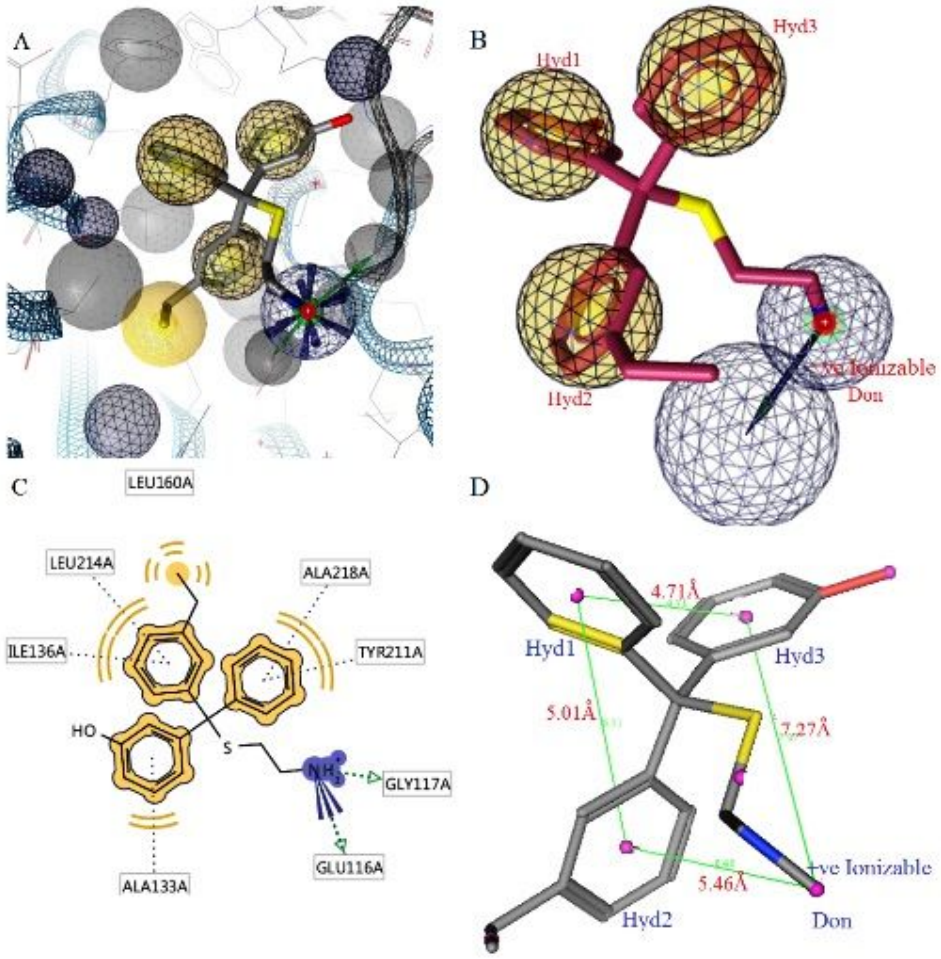
A
B
Hyd3
Hyd1
Hyd2
ve Ionizable
Don
C
LEU160A
D
LEU214A
ALA218A
ILE136A
TYR211A
HO
S
GLY117A
GLU116A
ALA133A
4.71Å
Hyd1
Hyd3
5.01Å
7.27Å
5.46Å
+ve Ionizable
Hyd2
Don

(I)

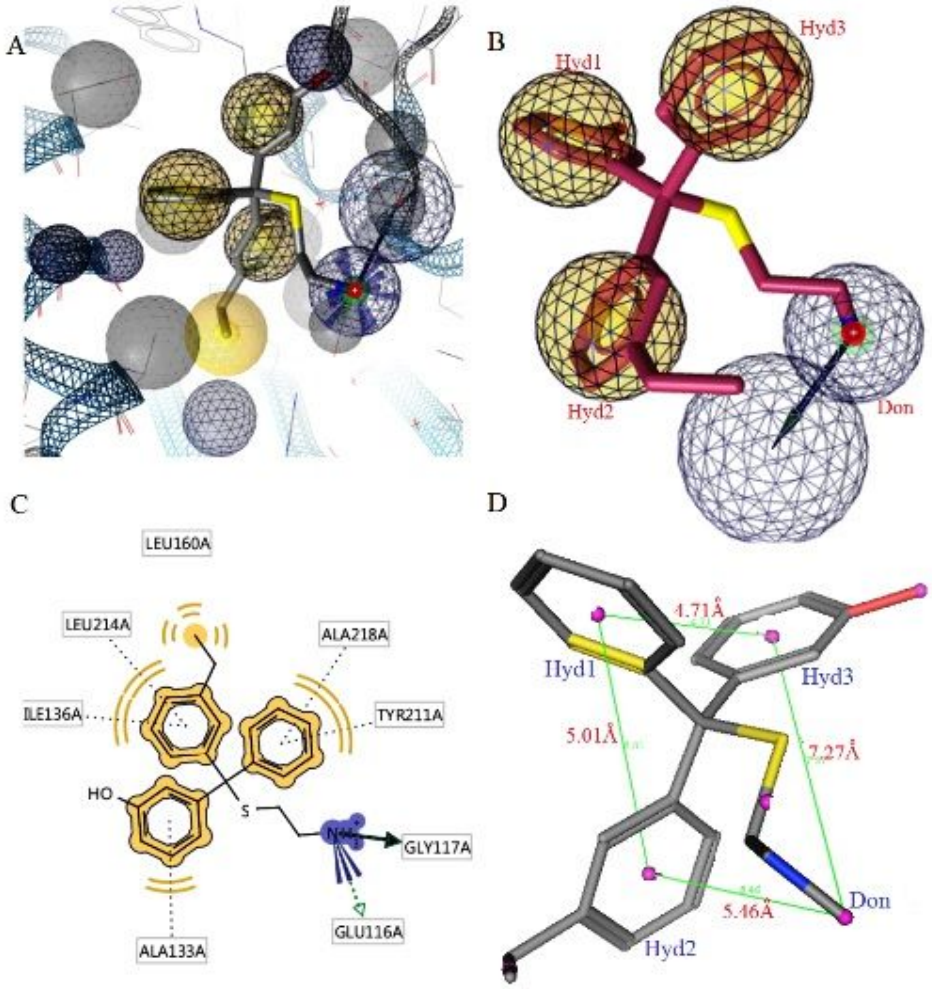
A
B
Hyd1
Hyd3
Hyd2
Don
C
D
LEU160A
LEU214A
ALA218A
ILE136A
TYR211A
HO
S
GLY117A
GLU116A
ALA133A
4.71Å
Hyd1
Hyd3
5.01Å
7.27Å
5.46Å
Don
Hyd2

(II)

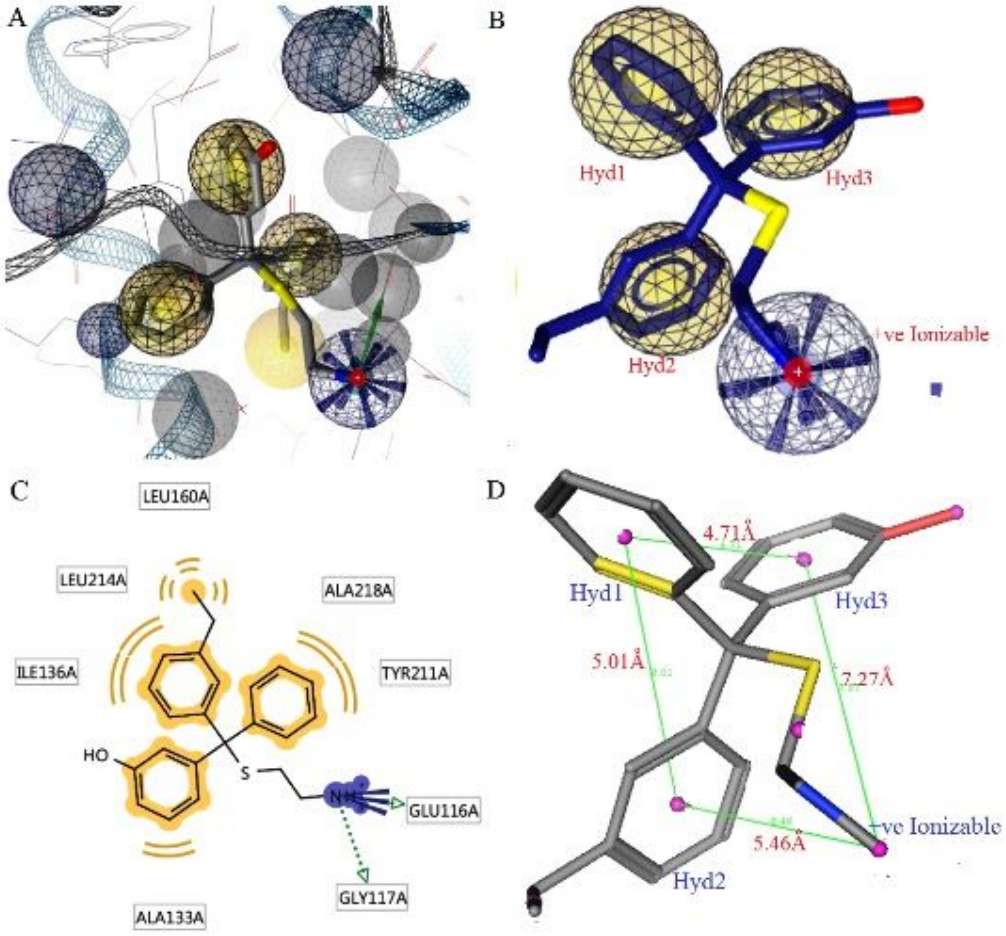

(III)

Figure S4. (I) 4BBG Model I, (II) 4BBG Model II, (III) 4BBG Model III

Pharmacophore models used to screen for potential active compounds against the 4BBG target; (A) projected within the target site, (B) with highlighted pharmacophore features located on atomic centers of the native ligand, H-bond donors and acceptors in blue and hydrophobic centers in yellow, (C) interactions between native ligand and target site amino acid residues, with hydrophobic interactions shown in light brown, H-bond donor interactions with the native ligand in green and acceptor interactions in red, (D) locations of centers of pharmacophore features on the native ligand showing distances between the centers, with distance measurements shown in red.

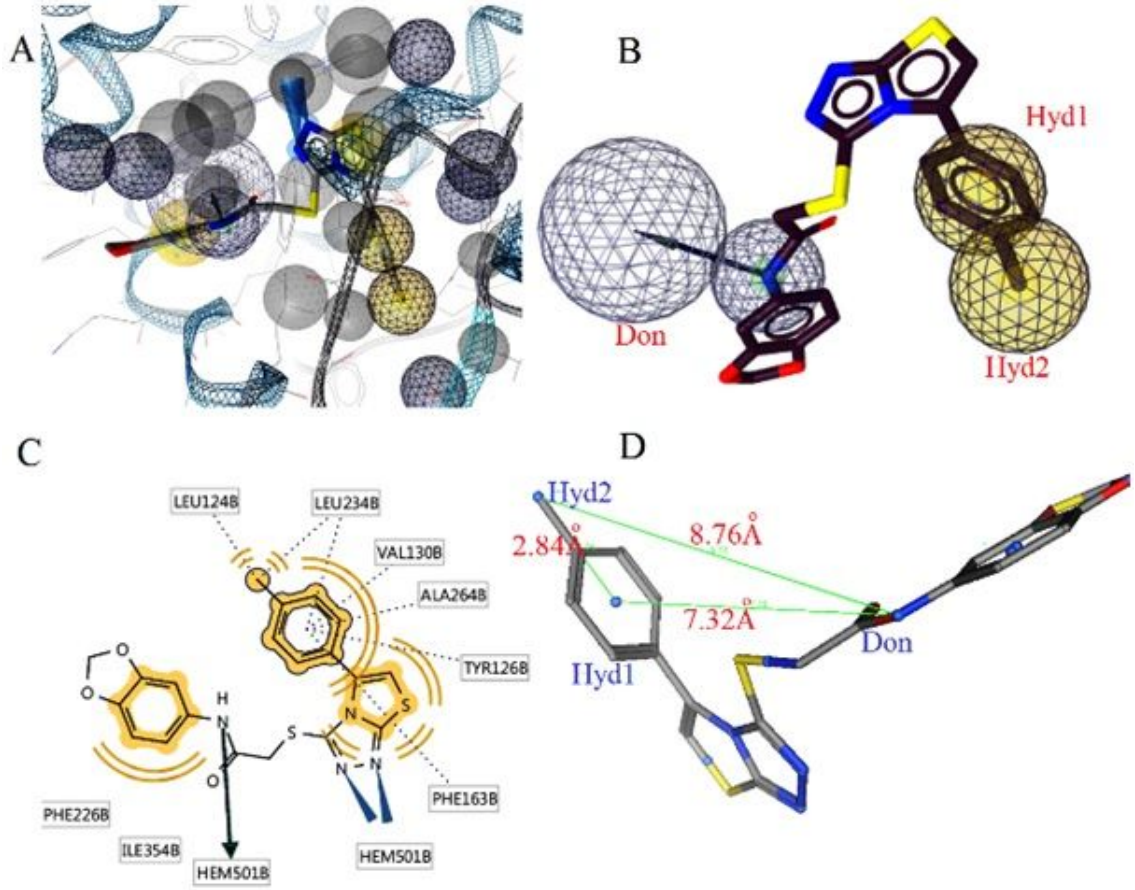
A
B
Hyd1
Don
Hyd2
C
D
LEU124B
LEU234B
VAL130B
ALA264B
TYR126B
PHE163B
PHE226B
ILE354B
HEM501B
HEM501B
Hyd2
2.84Å
8.76Å
7.32Å
Don
Hyd1

(I)

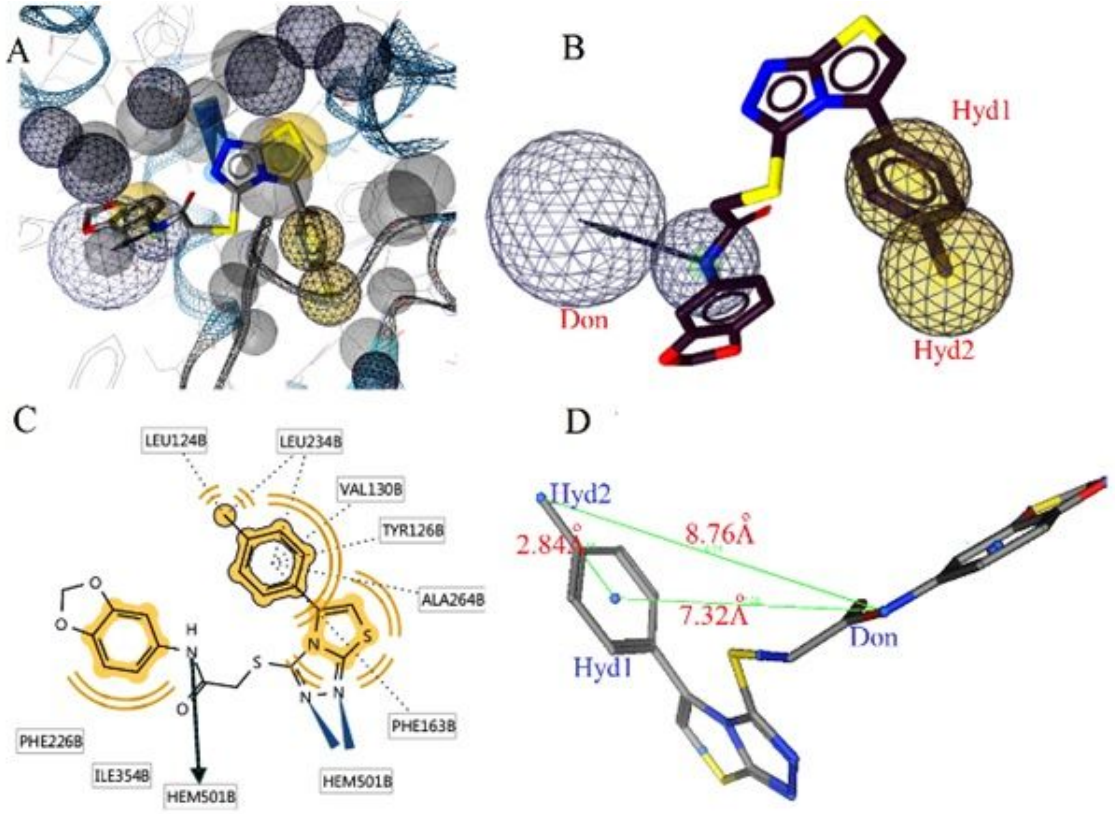

(II)

Figure S5. (I) 4PK5 Model I, (II) 4PK5 Model II

Pharmacophore models used to screen for potential active compounds against the 4PK5 target; (A) projected within the target site, (B) with highlighted pharmacophore features located on atomic centers of the native ligand, H-bond donors and acceptors in blue and hydrophobic centers in yellow, (C) interactions between native ligand and target site amino acid residues, with hydrophobic interactions shown in light brown, H-bond donor interactions with the native ligand in green and acceptor interactions in red, (D) locations of centers of pharmacophore features on the native ligand showing distances between the centers, with distance measurements shown in red.